Glutamate optimizes enzymatic activity under high hydrostatic pressure in *Desulfovibrio* species: effects on the ubiquitous thioredoxin system

Gaussier H[1#], Nouailler M[2#], Champaud E[1], Garcin E. B[2], Sebban-Kreuzer C[2], Bornet, O[3], Garel M[1], Tamburini C[1], Pieulle L[4], Dolla A[1]* and Pradel N[1]*

1. Aix Marseille Univ, Université de Toulon, CNRS, IRD, MIO, Marseille, France
2. Aix Marseille Univ, CNRS, LISM, Marseille, France
3. Aix Marseille Univ, CNRS, IMM, Marseille, France
4. Aix Marseille Univ, CNRS, LCB, Marseille, France

both authors contribute equally to this work
* To whom correspondence should be sent:
Alain Dolla : Email: alain.dolla@mio.osupytheas.fr
Nathalie Pradel; Email: nathalie.pradel@ird.fr

ABSTRACT

In piezophilic microorganisms, enzymes are optimized to perform under high hydrostatic pressure. The two major reported mechanisms responsible for such adaptation in bacterial species are changes in amino acids in the protein structure, favoring their activity and stability under high-pressure conditions, and the possible accumulation of micromolecular co-solutes in the cytoplasm. Recently, the accumulation of glutamate in the cytoplasm of piezophilic *Desulfovibrio* species has been reported under high pressure growth conditions. In this study, analysis of the effect of glutamate on the enzymatic activity of the thioredoxin reductase/thioredoxin enzymatic complex of either a piezosensitive or a piezophilic microorganism confirms its role as a protective co-solute. Analysis of the thioredoxin structures suggests an adaptation both to the presence of glutamate and to high hydrostatic pressure in the enzyme from the piezophilic strain. Indeed, the presence of large surface pockets could counterbalance the overall compression that occurs at high hydrostatic pressure to maintain enzymatic activity. A lower isoelectric point and a greater dipolar moment than that of thioredoxin from the piezosensitive strain would allow the protein from the piezophilic strain to compensate for the presence of the charged amino acid glutamate to interact with its partner.

KEYWORDS: hydrostatic pressure, co-solute, glutamate, thioredoxin.

INTRODUCTION

High hydrostatic pressure impacts all cellular components of microorganisms and modifies the activity of numerous key processes, such as enzymatic activities, eventually leading to the cell death of piezosensitive organisms (Abe 2007). As a general rule, secondary and tertiary structures of proteins remain stable at hydrostatic pressures below 500 MPa (Robinson and Sligar 1995). Within the physiologically relevant pressure range, the most important pressure effect is on the solvation of the core protein, which is enhanced with increasing hydrostatic pressure, leading to protein inactivation (Robinson and Sligar 1994; Robinson and Sligar 1995). Hydrostatic pressure may also induce protein-protein complex dissociation by weakening electrostatic and hydrophobic contacts which stabilize the complex (Gross and Jaenicke 1994). However, enzymes of high-pressure-adapted bacteria have been found to be more functional under high-pressure conditions than at atmospheric pressure (Le Bihan et al. 2013). Only a few enzymatic activities of piezophilic microorganisms have been studied. Regarding the 3-isopropylmalate dehydrogenase of *Shewanella bentica,* pressure adaptation has been attributed to a single amino acid substitution affecting the activity of the enzyme by modifying water molecule penetration into the active site, thus decreasing the hydration structure of the enzyme at high hydrostatic pressure (Hamajima et al. 2016). Dynamic simulations of the dihydrofolate reductase of *Moritella profunda* have indicated that atomic fluctuations of the loops, which are important for enzyme function, were increased with pressure by weakening hydrogen bonds (Huang et al. 2019). These intrinsic molecular adaptations have led to proteins that are more resistant to high hydrostatic pressure than their shallow-water counterparts (Yancey and Siebenaller 2015).

Another important finding in piezophilic organisms is the cellular accumulation of micromolecular osmolyte-type co-solutes, called “piezolytes” (Martin et al. 2002), that counteract the pressure effect, corresponding to extrinsic adaptation (Yancey and Siebenaller 2015). For example, trimethylamine N-oxide (TMAO), a well-known osmolyte suspected to interact indirectly with the protein through the surrounding water (Fedotova et al. 2017), has been reported in marine eukaryotes (Yancey et al. 2015). β-Hydroxybutyrate has been shown to accumulate at 20-30 MPa in *P. profundum* (Martin et al. 2002), and similarly, the intracellular concentration of ectoine has been shown to increase with pressure in *Alcanivorax borkumensis* (Scoma et al. 2016).

The role of piezolytes is to aid in maintaining protein function as well as macromolecule interactions within the cell at high hydrostatic pressure. The mechanism of action of these molecules is still largely unknown, but one can imagine that they act on protein solvation by helping to resist pressure-driven water penetration in the protein/complex core (Sarma and Paul 2013). It has been proposed that stabilization of proteins by ectoine is linked to its high hydration and exclusion from the water-protein interface. According to the Le Chatelier principle, this should tend toward a minimization of the area

of the water-protein interface obtained when the protein is in its native state and thus stabilizes the native structure through the "preferential exclusion model" (Arakawa and Timasheff 1985; Eiberweiser et al. 2015). Among the co-solutes of interest, glutamate has been shown to intracellularly accumulate in piezophilic *Desulfovibrio* species, *D. piezophilus* and *D. hydrothermalis*, under high hydrostatic pressure up to 100 mM and 200 mM at 26 MPa for *D. piezophilus* and *D. hydrothermalis*, respectively (Amrani et al. 2014; Amrani et al. 2016). On the other hand, neither the biosynthesis pathways of ectoine nor that of TMAO are present in the genomes of these strains. Glutamate has also notably been shown to be important for osmoregulation and survival during osmotic stress in several bacterial species (Saum and Müller 2007; Kang and Hwang 2018).

To better understand the effects of glutamate in the cell, we analyzed the structure of the model enzyme thioredoxin and the effect of glutamate on its activity at high hydrostatic pressure. Thioredoxins are small thiol:disulfide oxidoreductases (~12 kDa) ubiquitous in all domains of life that play a central role in the control of the thiol/disulfide redox balance of the cytoplasm as part of the NADPH-dependent thioredoxin reductase (TR)/thioredoxin (Trx) system. They have a highly conserved fold consisting of a central β-sheet surrounded by four α-helices and an active site with two cysteine residues that specify the biological activity of the protein (Martin 1995). Our study specifies the effect of glutamate on the enzymatic activity of TR/Trx complexes from the piezophile *Desulfovibrio piezophilus* C1TLV30 and the piezosensitive *Desulfovibrio vulgaris* Hildenborough sulfate reducers (Pieulle et al. 2011). This study shows that the structure of the TR/Trx system from piezophilic species is adapted to the presence of glutamate. Factors of this adaptation are discussed in light of the NMR structure of the *D. vulgaris* thioredoxin solved for this study and the structural modeling of the *D. piezophilus* thioredoxin.

MATERIALS AND METHODS

Cloning of *D. piezophilus* C1TLV30^T TR/Trx system. BN4v2_10319 (*trx1*) and BN4v2_10320 (*trB*) coding sequences were amplified by PCR by using the Taq-& LOAD™ Mastermix 5xC (MP Biomedicals Europe), with *D. piezophilus* C1TLV30 genomic DNA (GenBank accession n°FO203427) as the template, using primers pairs *trx1*-10319-fwHis and *trx1*-10319-rev, and *trB*-10320-fwHis and *trB*-10320-rev, respectively. Forward and reverse oligonucleotide primer sequences are listed in Table 1. A cloning procedure was designed to introduce one N-terminal His-tag as already published (Pieulle et al. 2011). The resulting amplicon was purified using the Wizard SV Gel and PCR Clean-Up System from Promega and digested with the appropriate restriction enzymes purchased from New England Biolabs (Table 1). The *trx1* and *trB* amplicons were cloned into pJF119EH and the vector was screened by PCR using

primers p119+ and p119-, as previously described (Pieulle et al. 2011), to generate plasmids p319 and p320, respectively.

Protein production and purification. *E. coli* TG1 was used for heterologous expression of both TR- and Trx-encoding genes as previously described (Pieulle et al. 2011). Recombinant *E. coli* TG1 strains were grown in either Luria-Bertani (LB), 2YT, or M9-glucose medium (Sambrook et al. 1989) with ampicillin (100 μg/mL). For *D. piezophilus* C1TLV30 Trx1 (DpTrx1) production, *E. coli* TG1 (p139) was grown overnight in LB medium at 37 °C; this culture was used to inoculate 1 liter of 2YT medium (1% vol/vol). The culture was incubated at 37 °C until the optical density at 600 nm (OD_{600nm}) reached 0.6. DpTrx1 production was then induced by adding a final concentration of 0.5 mM isopropyl β-D-1-thiogalactopyranoside (IPTG). Cells were further grown for 4 h and harvested by centrifugation (20 min at 7,000 x g, 4 °C), and the pellet was stored at -80 °C. For *D. piezophilus* C1TLV30 TR (DpTR1) production, *E. coli* TG1 (p320) was grown overnight in LB medium at 37 °C; this culture was further used to inoculate 1 liter of M9-glucose medium (1% vol/vol). Cells were grown at 37 °C until the OD_{600nm} reached 0.8. TR production was then induced by adding a final concentration of 1 mM IPTG, and the cells were further grown for 16 h and then harvested by centrifugation (20 min at 7,000 x g, 4 °C). The pellet was stored at -80 °C. His-tagged DpTrx1 and DpTR1 were purified as previously described for DvTrx1 and DpTR1 (Pieulle et al. 2011). Production and purification of recombinant Trx1 (DvTrx1) and TR1 (DvTR1) from *D. vulgaris* Hildenborough was performed as previously described (Pieulle et al. 2011). The purity of the proteins was checked by SDS-PAGE on a 12.5% polyacrylamide gel using the Instant Blue (Coomassie Blue) staining procedure (Expedon, UK). Trx1 concentrations were measured using the Pierce BCA Protein Assay Kit (Thermo Scientific), and TR1 concentrations were calculated using the ε_{451nm} value of 11,300 $M^{-1}.cm^{-1}$.

Steady state kinetics analysis for optimization of the experiments at 0.1 MPa. The reaction mixture was composed of 0.1 M potassium phosphate buffer, pH 7.5, 2 mM EDTA, 1 mM DTNB, and 1 mM NADPH complemented with different volumes of sodium glutamate solution to reach a final concentration of 0, 10, 50, 100 or 500 mM glutamate for a final reaction volume of 200 µL. A final concentration of 10 µM Trx1 and 0.1 µM TR1 reductase from either *D. piezophilus* or *D. vulgaris* was added to initiate the reaction. As controls, water replaced the enzyme and/or glutamate. Kinetic experiments were recorded by measuring the optical density at 412 nm (OD_{412nm}) with a Shimadzu UV-1601 spectrophotometer under constant stirring. The DTNB reduction spectroscopic signal was converted into µM concentration by using the Beer-Lambert law ($\varepsilon^{DTNB}_{412nm}$=14,150 $M^{-1}.cm^{-1}$). Each experiment was performed in triplicate.

Enzymatic activity assays at 0.1 and 25 MPa. Reactions (200 μL final volume) were performed in 2 mL borosilicate glass syringes (Socorex Dosys, Swiss). For the experiments at 25 MPa, syringes were inserted into 250 mL-volume high-pressure bottles (HPBs), and the hydrostatic pressure was controlled using a manual manometer. A reaction mixture of 0.1 M potassium phosphate buffer, pH 7.5, 2 mM EDTA, 1 mM DTNB, and 1 mM NADPH was prepared with or without 100 mM glutamate. Each reaction mixture was separated into four 200 μL samples. For each pressure condition (0.1 and 25 MPa), one sample was prepared by adding 10 μM Trx1 and 0.1 μM TR1, and a control was prepared by replacing the enzymes with H_2O. All buffers, enzyme stocks and reactive were kept on ice. Incubations were performed at 0.1 or 25 MPa at 25 °C for 45 min. Then, the HPBs were quickly depressurized, and the OD_{412nm} of each reaction mixture was measured. OD_{412nm} of blank reactions were subtracted from the reaction sample OD_{412nm}, and the Beer-Lambert law was applied to calculate the molar quantity of DTNB hydrolyzed in 45 min ($\varepsilon^{DTNB}_{412nm}$=14,150 $M^{-1}.cm^{-1}$). Each experiment was performed in triplicate.

DvTrx1 structure calculation. The NMR sample contained 1 mM DvTrx1 (10% D_2O, 90% H_2O) in 50 mM phosphate buffer and 100 mM NaCl, pH 5.5. The spectra were analyzed with CARA (Keller 2004) based on the resonance assignment previously deposited at the BMRB under accession code 17299. For structure calculations, 84 restraints were used for backbone hydrogen bonds, 170 backbone φ and ψ dihedral restraints derived from TALOS (Cornilescu et al. 1999) and 2071 nOe (nuclear Overhauser effect). The 20 lowest energy structures were water refined using the Amber 4.1 force field. The structural coordinates have been deposited in the Protein Data Bank under accession number 6ZOM.

DpTrx1 structural model. A homology model of oxidized DpTrx1 was generated with the Swiss-Model server (Waterhouse et al. 2018) based on the template structure of the oxidized thioredoxin DvTrx1 (pdb 6ZOM). The internal cavities and the ribbon models were generated with PyMOL (PyMOL Molecular Graphics System, Version 2.0 Schrödinger, LLC). Volume cavities were measured with the CastP server, with a radius probe of 0.9 Å (Tian et al. 2018) and with Void protein (Cuff and Martin 2004). Electrostatic potentials were calculated with the APBS module of PyMOL.

Data Analysis. Statistical analyses were performed with XLSTAT (Addinsoft) using the Student's t-test. Values were considered different at the α=0.01 significance level.

RESULTS and DISCUSSION

Sequence properties of the *D. piezophilus* thioredoxin system. *D. piezophilus* Trx1, encoded by the *trx1* gene (BN4v2_10319), contained the classical WCGPC active site motif; in addition, the two residues Asp-24 and Lys-55, found in Trx1 of the piezosensitive *D. vulgaris* Hildenborough strain, that have been suggested to deprotonate Cys-32 and to contribute to proton uptake accompanying the reduction of Trx1 (Pieulle et al. 2011), were conserved in DpTrx1 (Fig. 1a). Amino acid sequence alignment of DpTrx1 and DvTrx1 showed 84 identical residues (78.50%), 10 strongly similar residues (9.35%), 5 weakly similar residues (4.67%) and 8 different residues (7.48%) (Fig. 1a). The thioredoxin reductase of *D. piezophilus* C1TLV30, encoded by the *trB* gene (BN4v2_10320), exhibited the signature motifs VxxxHRRDxxRA and GGGxxAxE required for NADPH binding and the GR/KG and FF motifs for the thioredoxin binding site and the CxxC active site (Fig. 1b). These sequence elements show that the thioredoxin reductase of *D. piezophilus* C1TLV30 belongs to the TR1 group, as defined by Valette and coworkers (Valette et al. 2017). Overall, these findings show that the *D. piezophilus* C1TLV30 genome encodes one classical TR/Trx system homologous to the *D. vulgaris* Hildenborough TR1/Trx1 system.

Comparative enzymatic activities of the thioredoxin systems: DTNB reduction by the TR1/Trx1 complexes from *D. piezophilus* C1TLV30 and *D. vulgaris* Hildenborough was studied at both atmospheric pressure (0.1 MPa) and high hydrostatic pressure (25 MPa), with or without 100 mM glutamate (Fig. 2). Experiments were based on final DTNB reduction over a 45 min time period. In the absence of glutamate, the amounts of DTNB reduced by the *D. piezophilus* TR1/Trx1 complex were higher at 25 MPa (29.4 ± 6.4 µM) than at 0.1 MPa (5.8 ± 2.4 µM) (p-value<0.01) (Fig. 2a). The activity of the *D. vulgaris* TR1/Trx1 complex was higher at atmospheric pressure than at 25 MPa (36.4 ± 4.5 µM *versus* 15.1 ± 4.6 µM of reduced DTNB, respectively (p-value<0.01)) (Fig. 2b). Thus, both complexes showed the highest activity under the hydrostatic pressure that the cells usually encounter, *i.e.,* high hydrostatic pressure for *D. piezophilus* and atmospheric pressure for *D. vulgaris*. When the complexes were placed under unfavorable hydrostatic pressure for the corresponding cells, their activity was lower, as the *D. piezophilus* TR1/Trx1 complex lost 85% of its activity at 0.1 MPa, and the *D. vulgaris* TR1/Trx1 complex lost 58% of its activity at 25 MPa. This shows that the *D. piezophilus* TR1/Trx1 complex is adapted to high hydrostatic pressure conditions, in agreement with the piezophilic nature of *D. piezophilu*s C1TLV30, while the *D. vulgaris* TR1/Trx1 complex is better adapted to atmospheric pressure, in agreement with the piezosensitive nature of *D. vulgaris* Hildenborough.

To assess the effect of glutamate as pressure co-solute, the activities of both TR1/Trx1 complexes were measured in the presence of glutamate. To first evaluate the diffusion effect of the substrate toward the enzymes, the initial velocity under steady-state conditions for DTNB reduction by the *D. vulgaris* TR1/Trx1 complex was measured at different glutamate concentrations under constant stirring (Fig. 3). No significant change in the initial velocity was recorded from 0 to 100 mM glutamate (p-

value>0.01), meaning that the increase in density due to glutamate could be easily compensated by gentle mechanical stirring. When the glutamate concentration increased to 500 mM, the velocity decreased from approximately 8 µM.min^{-1} to 6 µM.min^{-1}. It should be noted that the pH (~7.5) was not modified by the addition of glutamate until 100 mM and slightly increased to 7.8 in the presence of 500 mM glutamate. The decrease of approximately 20% in the velocity in the presence of 500 mM glutamate may thus be related to a decrease in the capacity of the substrate to diffuse through this viscous environment, despite constant stirring. Since intracellular glutamate accumulation was estimated at approximately 100 mM in *D. piezophilus* cells grown at 26 MPa (Amrani et al. 2014) and since our results showed a very close kinetic behavior from 0 to 100 mM glutamate and therefore no inhibitory effect, this latter concentration was kept for further experiments.

In the presence of 100 mM glutamate, the amount of DTNB reduced by the *D. piezophilus* TR1/Trx1 complex increased significantly at 0.1 MPa, from 4.4 ± 2.4 µM without glutamate to 21.6 ± 6.5 µM with glutamate (p-value<0.01) (Fig. 2a). In contrast, no significant difference in the activity of the *D. vulgaris* TR1/Trx1 complex at 0.1 MPa was observed with or without glutamate (Fig. 2b). At 25 MPa, an upward trend in the activity of the *D. piezophilus* TR1/Trx1 complex in the presence of glutamate was noticed (37.1 ± 6.9 µM versus 29.4 ± 6.4 µM of reduced DTNB with and without glutamate, respectively) (Fig. 2a). Similarly, an increase in the amount of DTNB reduced by the *D. vulgaris* TR1/Trx1 complex was observed in the presence of 100 mM glutamate (43.7 µM versus 15.1 µM without glutamate (mean values)) (Fig. 2b). However, the standard deviations observed for the experiments performed with the *D. piezophilus* TR1/Trx1 complex in the presence of glutamate at both 0.1 and 25 MPa were much lower than those obtained with the *D. vulgaris* TR1/Trx1 complex. It should be noted that these experiments were performed using a single point activity measurement after 45 min of incubation without stirring and thus were highly dependent on the turnover of the enzymes. Because the largest standard deviations were observed for the Dv TR1/Trx1 complex in the presence of glutamate, it suggests that this latter affects especially the turnover of this enzymatic system. To understand this effect, the structures of the Trx1 from both species were determined.

Structures of *DvTrx1 and DpTrx1*.

To obtain more insights into the structural adaptation of the *D. piezophilus* TR1/Trx1 complex to high hydrostatic pressure and to the presence of glutamate, comparison of the three-dimensional structure of the thioredoxins from *D. vulgaris* Hildenborough and *D. piezophilus* C1TLV30 was performed. First, the three-dimensional structure of DvTrx1 in the oxidized state was determined. The resulting ensemble of solutions, consisting of the 20 lowest energy structures of DvTrx1, adopted a typical thioredoxin fold: a five-stranded twisted central β-sheet surrounded by four α-helices, with α2 and α4 helices on one side and α1 and α3 helices on the opposite side (Fig. 4a). The N-terminal motif

244 β1α1β2α2β3 was connected by the loop comprising the α3 helix to the C-terminal motif β4β5α4. The
245 active site (CGPC) was formed by a protruding loop between strand β2 and the N-terminus of helix α2.
246 The proline of the catalytic site generated a distortion in the α2 helix, separating the CGPC consensus
247 from the rest of the helix. The electrostatic surface of DvTrx1 exhibited a charge repartition similar to
248 that of canonical thioredoxins. Overall, the protein displayed high three-dimensional similarities to
249 known thioredoxins such as *E. coli* Trx1 (Katti et al. 1990).
250 The homology model of DpTrx1, performed with the Swiss model, indicated a global model quality
251 estimation (GMQE) of 0.66/1.00, resulting in good reliability of the model (Fig. 4b). Only 0.4 Å rmsd
252 was evidenced between both thioredoxin three-dimensional structures, resulting in a typical
253 thioredoxin fold of DpTrx1. Interestingly, the less conserved part of the protein was localized at the
254 opposite side of the active site, in the α1 helix, which contained 2 additional glutamic acid residues at
255 positions 13 and 18 that were replaced by serine and alanine, respectively, in DvTrx1. Two additional
256 acidic residues were also found in DpTrx1: a glutamic acid at position 45 in the α2 helix, replaced by
257 alanine in DvTrx1, and an aspartic acid at position 81, replaced by asparagine in DvTrx1 (Fig. 4a-d) (Fig.
258 1a). These structural features confer a more acidic calculated isoelectric point (pI = 5.0 for DpTrx1
259 *versus* 4.6 for DvTrx1) and a different dipolar moment, 21.4° angle deviation and +104 Debyes for
260 DpTrx1 (Fig. 4e). In addition, DpTrx1 had larger surface pockets than DvTrx1 (2003.5 $Å^3$ *versus* 1878.5
261 $Å^3$, respectively). Overall, the structure of DpTrx1 was 2% larger than that of DvTrx1.
262 This structural comparison revealed two way of adaptation of DpTrx1. First, the surface pockets, which
263 are larger than those in DvTrx1, could be compressed to compensate for the lack of flexibility under
264 high pressure in the region of the cysteines. Second, the larger number of acidic residues in DpTrx1
265 compared to DvTrx1 could be linked to the adaptation of the protein sequence to the presence of
266 glutamate in the cytoplasm of the cell; the resulting dipolar moment of the protein would
267 counterbalance its presence by conferring an optimal orientation of Trx1 for TR1/Trx1 complex
268 formation.
269 It can be postulated that glutamate protects the protein core from pressure-driven water penetration
270 and thus stabilizes the native conformation of the protein through either the “preferential exclusion
271 model” (Arakawa and Timasheff 1985) or the “water replacement theory” (Crowe et al. 1990), which
272 proposes that the molecule binds directly to the protein by replacing water molecules in the hydration
273 shell of the protein. The activity of the TR1/Trx1 complex of *D. piezophilus* was greater at atmospheric
274 pressure in the presence of glutamate than without glutamate, supporting the concept that the
275 enzymes have adapted to the hydrostatic pressure and thus to the presence of glutamate, as glutamate
276 accumulates at high hydrostatic pressure (Amrani et al. 2014). Structure of *D. piezophilus* Trx1
277 highlights peculiar features like a larger structure and surface pockets than its homologous protein

isolated from the piezosensitive *Desulfovibrio vulgaris* strain. This could counterbalance the overall compression that occurs at high hydrostatic pressure to maintain enzymatic activity. Additionally, *D. piezophilus* Trx1 exhibits a relatively lower isoelectric point and a more pronounced dipolar moment than those of DvTrx1, which could allow for the protein to compensate for the presence of intracellular glutamate to interact with its partner. Altogether, the enzymatic data and the structural analysis of Trx1 allow us to conclude that the Dp TR1/Trx1 system may be adapted to the presence of glutamate, as opposite to the Dv TR1/Trx1 system. On a physiological point of view, antioxidant defense mechanism has been shown to be an important mechanism to cope with high hydrostatic pressure in the deep-sea bacterium *Shewanella piezotolerans* WP3 (Xie et al. 2018). In the same way, the TR1/Trx1 complex plays a key role in maintaining the redox homeostasis in the cell (Pieulle et al. 2011). Adaptation of the *D. piezophilus* TR1/trx1 to the presence of glutamate is thus an advantage to maintain antioxidant defense mechanism active under high hydrostatic pressure.

Overall, these data pointed out the protective role of glutamate in maintaining the enzymatic activity of the TR1/Trx1 complex. Thus, adaptation to high hydrostatic pressure appears to be a complex mechanism involving glutamate overproduction to protect the cell and the enzyme from pressure, and structural changes to adapt to both hydrostatic pressure and the presence of glutamate.

Aknowledgement : This is a post-peer-review, pre-copyedit version of an article published in Extremophiles. The final authenticated version is available online at: https://dx.doi.org/10.1007/s00792-021-01236-x.

299

300 **REFERENCES**

301 Abe F (2007) Exploration of the effects of high hydrostatic pressure on microbial growth, physiology
302 and survival: perspectives from piezophysiology. Biosci Biotechnol Biochem 71:2347-2357 doi:
303 10.1271/bbb.70015

304 Amrani A, Bergon A, Holota H, Tamburini C, Garel M, Ollivier B, Imbert J, Dolla A, Pradel N (2014)
305 Transcriptomics reveal several gene expression patterns in the piezophile *Desulfovibrio*
306 *hydrothermalis* in response to hydrostatic pressure. PLoS One 9:e106831 doi:
307 10.1371/journal.pone.0106831

308 Amrani A, van Helden J, Bergon A, Aouane A, Ben Hania W, Tamburini C, Loriod B, Imbert J, Ollivier B,
309 Pradel N, Dolla A (2016) Deciphering the adaptation strategies of *Desulfovibrio piezophilus* to
310 hydrostatic pressure through metabolic and transcriptional analyses. Environ Microbiol Rep
311 8:520-526 doi: 10.1111/1758-2229.12427

312 Arakawa T, Timasheff SN (1985) The stabilization of proteins by osmolytes. Biophys J 47:411-414 doi:
313 10.1016/S0006-3495(85)83932-1

314 Cornilescu G, Delaglio F, Bax A (1999) Protein backbone angle restraints from searching a database for
315 chemical shift and sequence homology. J Biomol NMR 13: 289-302 doi:
316 10.1023/a:1008392405740

317 Crowe JH, Carpenter JF, Crowe LM, Anchordoguy TJ (1990) Are freezing and dehydration similar stress
318 vectors? A comparison of modes of interaction of stabilizing solutes with biomolecules.
319 Cryobiology 27:219-231 doi: 10.1016/0011-2240(90)90023-w

320 Cuff AL, Martin AC (2004) Analysis of void volumes in proteins and application to stability of the p53
321 tumour suppressor protein. J Mol Biol 344: 1199-1209 doi: 10.1016/j.jmb.2004.10.015

322 Eiberweiser A, Nazet A, Kruchinin SE, Fedotova MV, Buchner R (2015) Hydration and ion binding of the
323 osmolyte ectoine. J Phys Chem B 119:15203-15211 doi: 10.1021/acs.jpcb.5b09276

324 Fedotova M, Kruchinin S, Chuev G (2017) Hydration structure of osmolyte TMAO:
325 concentration/pressure-induced response. New J Chem 41:1219-1228 doi:
326 10.1039/C6NJ03296F

327 Gross M, Jaenicke R (1994) Proteins under pressure. The influence of high hydrostatic pressure on
328 structure, function and assembly of proteins and protein complexes. Eur J Biochem 221:617-
329 630 doi: 10.1111/j.1432-1033.1994.tb18774.x

330 Hamajima Y, Nagae T, Watanabe N, Ohmae E, Kato-Yamada Y, Kato C (2016) Pressure adaptation of 3-
331 isopropylmalate dehydrogenase from an extremely piezophilic bacterium is attributed to a
332 single amino acid substitution. Extremophiles 20:177-186 doi: 10.1007/s00792-016-0811-4

333 Huang Q, Rodgers J, Hemley R, Ichiye T (2019) Effects of pressure and temperature on the atomic
334 fluctuations of dihydrofolate reductase from a psychropiezophile and a mesophile. IJMS
335 20:1452-1465 doi: 10.3390/ijms20061452

336 Kang Y, Hwang I (2018) Glutamate uptake is important for osmoregulation and survival in the rice
337 pathogen *Burkholderia glumae*. PLoS One 13:e0190431 doi: 10.1371/journal.pone.0190431

338 Katti SK, LeMaster DM, Eklund H (1990) Crystal structure of thioredoxin from *Escherichia coli* at 1.68 A
339 resolution. J Mol Biol 212:167-184 doi: 10.1016/0022-2836(90)90313-B

340 Keller RLJ (2004) The computer aided resonance assignment tutorial. Cantina Verlag, Goldau,
341 Switzerland

342 Le Bihan T, Rayner J, Roy MM, Spagnolo L (2013) *Photobacterium profundum* under pressure: a MS-
343 based label-free quantitative proteomics study. PLoS One 8:e60897 doi:
344 10.1371/journal.pone.0060897

345 Martin D, Bartlett D, Roberts M (2002) Solute accumulation in the deep-sea bacterium *Photobacterium*
346 *profundum*. Extremophiles 6:507-514 doi: 10.1007/s00792-002-0288-1

347 Martin J (1995) Thioredoxin--a fold for all reasons. Structure 3:245-250 doi: 10.1016/s0969-
348 2126(01)00154-x

Pieulle L Stocker P, Vinay M, Nouailler M, Vita N, Brasseur G, Garcin E, Sebban-Kreuzer C, Dolla A (2011) Study of the thiol/disulfide redox systems of the anaerobe *Desulfovibrio vulgaris* points out pyruvate:ferredoxin oxidoreductase as a new target for thioredoxin 1. J Biol Chem 286:7812-7821 doi: 10.1074/jbc.M110.197988

Robinson CR, Sligar SG (1994) Hydrostatic pressure reverses osmotic pressure effects on the specificity of EcoRI-DNA interactions. Biochemistry 33:3787-3793 doi: 10.1021/bi00179a001

Robinson CR, Sligar SG (1995) Hydrostatic and osmotic pressure as tools to study macromolecular recognition. Methods Enzymol 259:395-427 doi: 10.1016/0076-6879(95)59054-4

Sambrook J, Fritsch E, F, Maniatis T (1989) Bacterial media, anitibiotics and bacterial strains. In: C N (ed) Molecular cloning. A laboratory manual. Second Edition. Cold Spring Harbor Laboratory Press, Cold Spring Harbor, pp A1-A13

Sarma R, Paul S (2013) Crucial importance of water structure modification on trimethylamine N-oxide counteracting effect at high pressure. J Phys Chem B 117:677-689 doi: 10.1021/jp311102v

Saum SH, Müller V (2007) Salinity-dependent switching of osmolyte strategies in a moderately halophilic bacterium: glutamate induces proline biosynthesis in *Halobacillus halophilus*. J Bacteriol 189:6968-6975 doi: 10.1128/JB.00775-07

Scoma A, Barbato M, Borin S, Daffonchio D, Boon N (2016) An impaired metabolic response to hydrostatic pressure explains *Alcanivorax borkumensis* recorded distribution in the deep marine water column. Sci Rep 6:31316 doi: 10.1038/srep31316

Tian W, Chen C, Lei X, Zhao J, Liang J (2018) CASTp 3.0: computed atlas of surface topography of proteins. Nucleic Acids Res 46:W363-W367 doi: 10.1093/nar/gky473

Valette O, Tran TTT, Cavazza C, Caudeville E, Brasseur G, Dolla A, Talla E, Pieulle L (2017) Biochemical function, molecular structure and evolution of an atypical thioredoxin reductase from *Desulfovibrio vulgaris*. Front Microbiol 8:1855 doi: 10.3389/fmicb.2017.01855

Waterhouse A, Bertoni M, Bienert S, Studer G, Tauriello G, Gumienny R, Heer FT, de Beer TAP, Rempfer C, Bordoli L, Lepore R, Schwede T (2018) SWISS-MODEL: homology modelling of protein structures and complexes. Nucleic Acids Res 46:W296-W303 doi: 10.1093/nar/gky427

Xie Z, Jian H, Jin Z, Xiao X (2018) Enhancing the Adaptability of the deep-sea bacterium *Shewanella piezotolerans* WP3 to high pressure and low temperature by experimental evolution under H2O2 stress. Appl Environl Microbiol 84:e02342-17 doi: 10.1128/AEM.02342-17

Yancey PH, Siebenaller JF (2015) Co-evolution of proteins and solutions: protein adaptation *versus* cytoprotective micromolecules and their roles in marine organisms. J Exp Biol 218:1880-1896 doi: 10.1242/jeb.114355

Figure Captions:

Fig. 1 Sequence alignment of a) the thioredoxin from *D. piezophilus* C1TLV30 (DpTrx1) and *D. vulgaris* Hildenborough (DvTrx1) (active site motif and residues important in the catalytic reaction are highlighted in gray) and b) the thioredoxin reductase from *D. piezophilus* C1TLV30 (DpTR1) and *D. vulgaris* Hildenborough (DvTR1) (conserved motifs for thioredoxin binding (Trx1 bind.), active site (Active site), pyrophosphate group of NAD(P)H binding (PP binding) and phosphate group of NADPH binding (2'P binding) are highlighted in gray). The alignments were generated using the ClustalW program from the IBPC server (npsa-prabi.ibcp.fr). Identical (*), strongly similar (:) and weakly similar (.) residues are indicated.

Fig. 2 Enzymatic activity assays at 0.1 and 25 MPa in the absence (white) or presence (gray) of glutamate. a) TR1/Trx1 complex from *D. piezophilus* C1TLV30; b) TR1/Trx1 from *D. vulgaris* Hildenborough. Mean values and error bars were obtained from at least 3 independent experiments. Significant differences between samples are indicated by an asterisk (Student's t-test, p-value<0.01)

Fig. 3 Initial velocity under steady-state conditions for DTNB hydrolysis by the TR1/Trx1 complex of *D. vulgaris* Hildenborough at various glutamate concentrations

Fig. 4 a) NMR Lower energy structure of oxidized DvTrx1 (active site WCPGC in ball and stick colored in gray, Sγ atoms in orange). b) Cartoon model of oxidized DpTrx1 (active site WCPGC in ball and stick colored in gray, Sγ atoms in orange); additional acidic functions compared to DvTrx1 are represented by red spheres. c) and d) Surface charges of DvTrx1 and DpTrx1, respectively. e) Superposition of DvTrx1 and DpTrx1 with their corresponding dipolar moments; angle variation is indicated

Fig. 1

a

```
                10        20        30        40        50        60
DpTrx1  MAHQITDGTFDQEVLQSEIPVLIDFWAPWCGPCRAMGPVIDELSEEYADQVKIVKMNVDE
DvTrx1  MAAQITDATFEASVLKSAIPVLIDFWAPWCGPCRAMGPVIDELAAEYEGKVLIVKMNVDD
        ** ****.**: .**:* ************************: ** .:* *******:

                70        80        90       100
DpTrx1  NSATPGKYGIRAIPTLILFKDGEVVDQSTGAVSKSSIKEMITKKAL-
DvTrx1  NPATPSKYGIRAIPTLILFKNGEVVEQVTGAVSKSSIKDMIAQKALG
        *.***.**************:****:* **********:**::***
```

b

```
                10        20        30        40        50        60
DpTR1   MKSYDAVVIGGGPAGMTAALYLLRAGVKTAMIEKLAPGGQVLMTAEIENYPGFPEGLQGW
DvTR1   MQQFDAIVIGGGPAGMTAALYLARSGVSVAMVERLSPGGQVLMTSEIENYPGFPKGIQGW
        *:.:**:*************** *:**..**:*:*:********:*********:*:***

                70        80        90       100       110       120
DpTR1   ELADKFAAHIENDELDRINDEVRSIELGTSLHTIHVGEQVVQTKMIILATGSRYRKLGIP
DvTR1   ELADLFAAHLEGYAITRFNDEVREIVPAPADNRVRVGDDWISGRTLILCSGARYKRLGLP
        **** ****:*.  : *:*****.*  ..: : ::**:: :. : :**.:*:**::**:*

                Trx1    Active  Trx1      PP binding          2'P binding
                bind.    site   bind.
                  130       140       150       160       170       180
DpTR1   GEERLLGKGVSYCALCDGNFFRGQDVAVIGGGNSALEEALYLARLVNKVYLIHRRDAFRG
DvTR1   DEERLTGKGVSYCALCDGNFFRGQVVGVVGGGNSALEESLYLSKLVKKLHLIHRRDDFRA
        .**** ****************** *.*:*********:***::**:*::****** **.

               190       200       210       220       230       240
DpTR1   LLCYQDKCLNHEKIEVVRNTVVNEIEGADEVESLALCNVKSKESSHLKIDAAFVFVGFEP
DvTR1   AKCYQDKVCIMPDIDVVRSSVVEAIHGDDRLTGVTVRNVKTGETSFLELDGLFIFIGFEP
          *****     .*:***.:**: *.* *.: .::: ***: *:*.*::*. *:*:****

              250       260       270       280       290       300
DpTR1   IMDFVPVEVERDKNG-IITDVEMRTNIPGVFAAGDIRSKLCRQVASAVGDGATAANAAFT
DvTR1   VGGFLPGGIERDEQGFVITDGEMRTNLPGIFAAGDIRSKMCRQVTTAVGDGATAANAAFV
        : .*:*  :***::* :*** *****:**:*********:****::**********.

DpTR1   YLQQFGI
DvTR1   YLEQLDA
        **:*:.
```

Fig 2

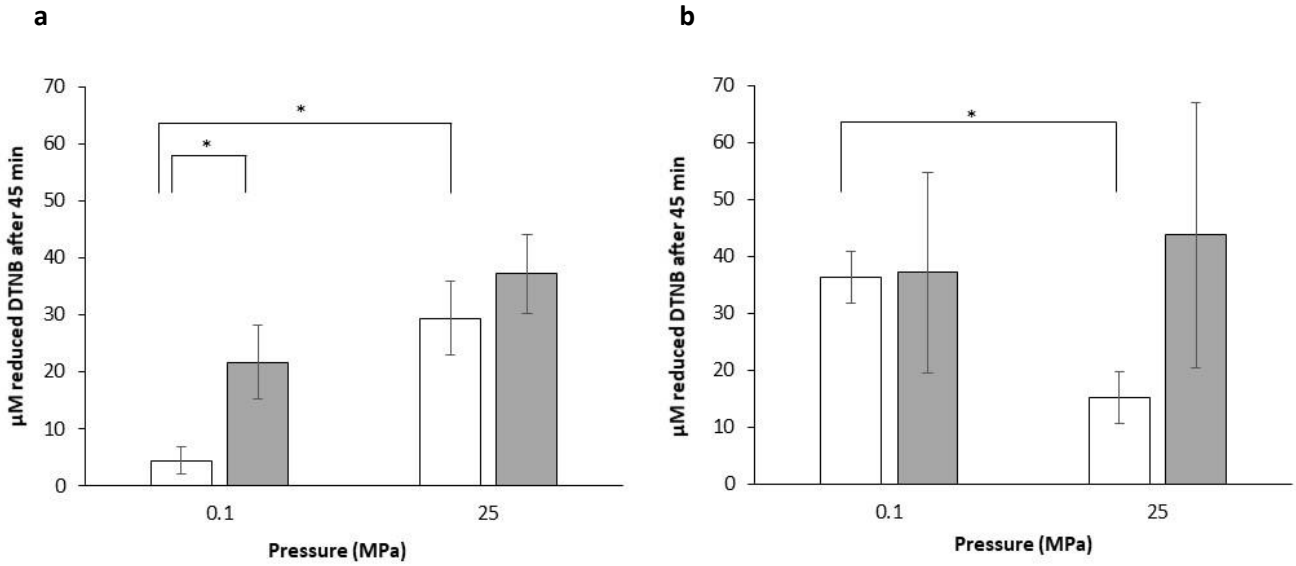
a
b
µM reduced DTNB after 45 min
70
60
50
40
30
20
10
0
*
*
0.1
25
Pressure (MPa)

Fig 3

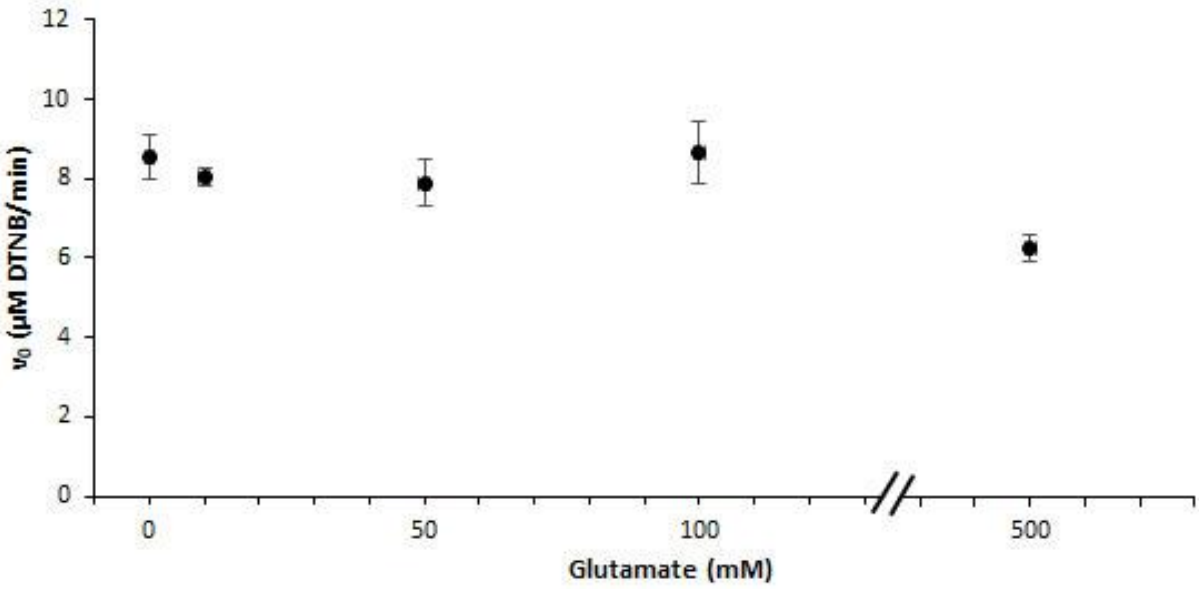

Fig 4

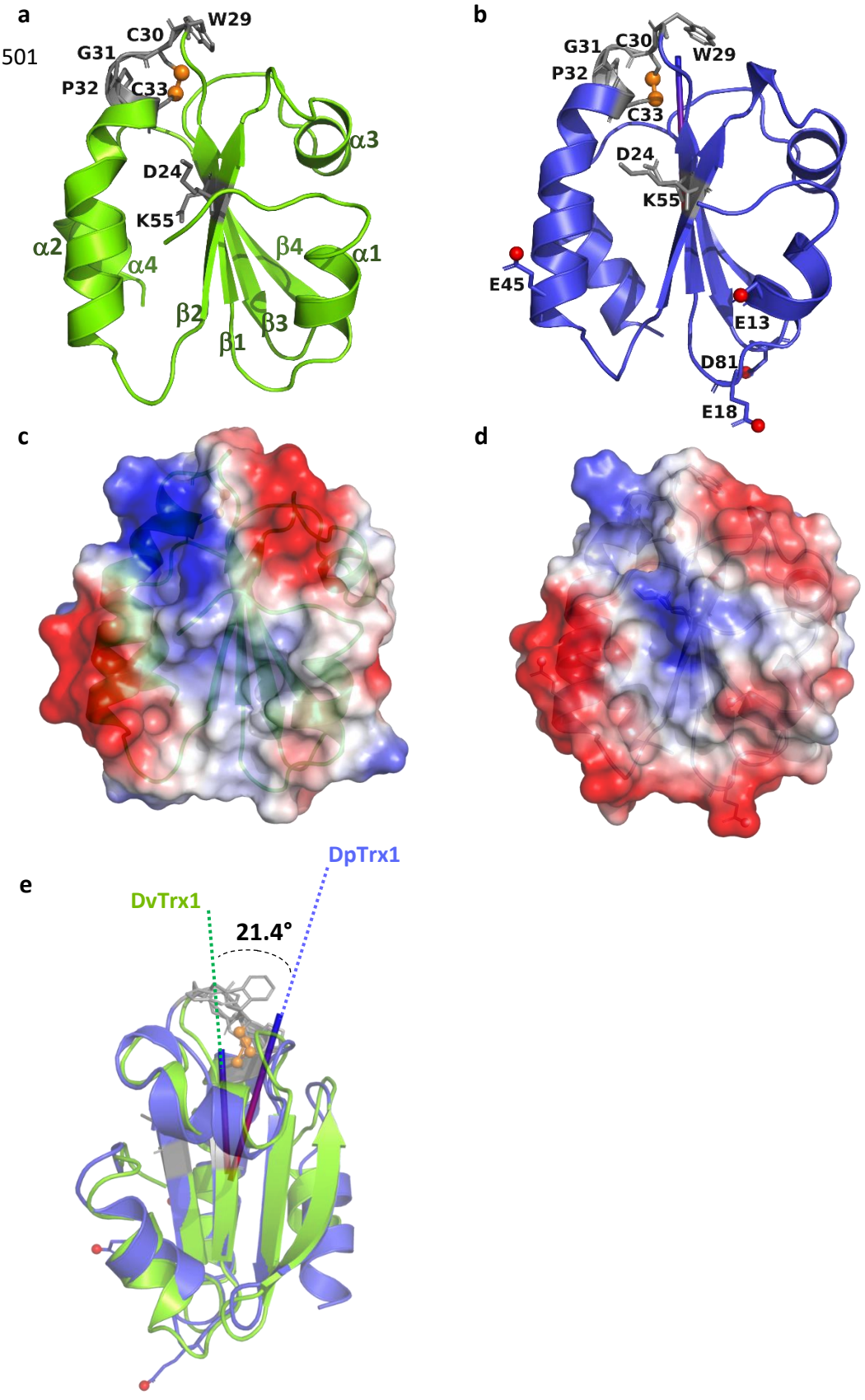
a
W29
C30
G31
P32
C33
α3
D24
K55
α2
α4
β4
α1
β2
β3
β1
b
G31
C30
W29
P32
C33
D24
K55
E45
E13
D81
E18
c
d
e
DpTrx1
DvTrx1
21.4°

TABLE 1: Oligonucleotide primers DNA sequence used for specific amplification and cloning of the *D. piezophilus* C1TLV30 TR1/Trx1system coding sequences.

Name	Sequence 5'-3'	Restriction enzyme
***trx1*-10319-fwHis**	GGGAATTCATG**CACCACCACCACCACCAC**GCACATCAGATTACGGAC	*Eco*RI
***trx1*-10319-rev**	TTGGATCCCTACAGCGCCTTCTTGGT	*Bam*HI
***trB*-10320-fwHis**	TTGAATTCATG**CACCACCACCACCACCAC**AAATCATATGACGCTGTA	*Eco*RI
***trB*-10320-rev**	TTGGATCCCTAAATACCGAACTGTTGG	*Bam*HI
p119 +	GTTCTGGCAAATATTCTGAAATG	
P119 -	GCTTCTGCGTTCTGATTTAAT	

The restriction enzyme recognition site is underlined in the sequence, and the six triplets encoding His-tagged domain for convenient purification are shown in boldface.

525